DOI: 10.21917/ijivp.2015.0151

# COMPARISON OF DIFFERENT SEGMENTATION ALGORITHMS FOR DERMOSCOPIC IMAGES

**A.A. Haseena Thasneem[1], R. Mehaboobathunnisa[2], M. Mohammed Sathik[3] and S .Arumugam[4]**
[1,2,3]*Department of Computer Science, Sadakathullah Appa College, India*
E-mail: [1]haseenajmal@gmail.com, [2]nisadiq8797@gmail.com, [3]mmdsadiq@gmail.com
[4]*Nandha Engineering College, India*
E-mail: principalnec@nandhainstitutions.org

***Abstract***

***This paper compares different algorithms for the segmentation of skin lesions in dermoscopic images. The basic segmentation algorithms compared are Thresholding techniques (Global and Adaptive), Region based techniques (K-means, Fuzzy C means, Expectation Maximization and Statistical Region Merging), Contour models (Active Contour Model and Chan - Vese Model) and Spectral Clustering. Accuracy, sensitivity, specificity, Border error, Hammoude distance, Hausdorff distance, MSE, PSNR and elapsed time metrices were used to evaluate various segmentation techniques.***

***Keywords:***

***Thresholding, Expectation Maximization, Contour Models, Dermoscopy, Spectral Clustering***

## 1. INTRODUCTION

Image segmentation is the process of partitioning a digital image into multiple regions or sets of pixels. This partitioning should be stopped when the object of interest in an application has been separated [1]. Accurate segmentation of medical images is very important for the analysis and diagnosis of abnormalities in different parts of the body. Segmentation becomes important since it further aids in classification of the segmented regions as benign or malignant. Malignancy insists the need for analysis like biopsy and thereafter medical excision. In order to avoid unnecessary biopsies, the need for accurate classification which is possible only by accurate segmentation techniques arises. It is not necessary that a segmentation algorithm suited for a particular medical image provides excellent results for other medical images also.

Dermatoscope is a non – invasive diagnostic technique which allows better visualization of surface and sub-surface skin structures. Dermoscopic images when interpreted for malignant melanoma diagnosis, consumes more time and is purely a subjective process even with trained dermatologists. The use of computer-aided diagnosis systems is of great assistance nowadays for untrained dermatologists. Even though many segmentation techniques are available in literature, the choice of segmentation algorithms used in this paper is based on popularity and simplicity of implementation.

Thresholding comes under similarity based approach [1] and can be subdivided into Global Thresholding and Adaptive (local) Thresholding. Global Thresholding is using a single threshold for the entire image whereas local thresholding partitions an image into several subimages with threshold defined for each subregion[2]. Thresholding methods perform fairly well if there is good contrast between the foreground and the background but not for images with no sharp peaks [3]. Also they require no prior knowledge of the image. The region based segmentation method used for comparison are the clustering algorithms, K means clustering developed by MacQueen [4] and Fuzzy C Means proposed by Bezdek [5]. Clustering is the process of grouping samples. The groups are called clusters. Both methods are iterative with the number of clusters defined by the user. For K means, the image pixels are divided among the clusters based on some distance metrics between the cluster centroids and all pixels. The cluster centroids are updated after each iteration and finally distance between the cluster centroids are maximized.

Fuzzy c-means is an unsupervised technique that finds application in feature analysis, clustering, and classifier designs. FCM is robust and retains more information from the original image than K means clustering. The main objective of FCM is to minimize an objective function iteratively by introducing certain fuzziness for the belongingness of each image pixel into each cluster [5], [6].The degree to which each pixel belongs to a region is given by the membership value. The crucial problem associated with clustering techniques is the assignment of number of clusters approximately by the user.

In an experiment, if all input parameters are known in prior then it is said to be a complete data case. Similarly, if any of the input parameters is unknown during the experimentation, then it is said to be an incomplete data case. The input variable which is unknown is termed as the hidden variable. The Expectation Maximization algorithm helps determining this hidden variable over multiple iterations. When it comes to an image segmentation context, the number of pixels and the number of clusters are known; but the cluster to which the pixel belongs is hidden. EM solves this uncertainty in two steps.

1) Expectation step - estimates the distribution of the hidden variable using the data and the current parameter values
2) Maximization step - maximizes the likelihood

In Statistical Region Merging, regions are sets of pixels with homogeneous properties and they are iteratively grown by combining smaller regions [7], [8]. This merging algorithm works with a statistical test which is based on a merging predicate and an order of merging.

Active Contour Models are parametric snake models proposed by Kass et al. [9] which locks onto the nearby edges under the influence of a user-imposed constrained energy (internal energy) and an energy of the image (external energy). Snake is a spline which is controlled by an energy minimizing function and relies on the image gradient for edge detection.

Chan - Vese model [10] for image segmentation overcomes the limitations of snake model by detecting concavities and contours with or without gradients. The representation and optimization of the energy functional is based on contour based gradient descent and Level-set based gradient descent respectively. This model detects even interior contours irrespective of the initial contour.

Spectral Clustering is the clustering of data points by considering them as connected subgraphs and not as distinct convex globular clusters as in K-means [11]. It uses the similarity between the data points represented using a similarity graph to cluster the input data. The similarity graph is associated with an adjacency/affinity matrix that gives the closeness between the data points. Points in the same cluster having high similarity and vice versa. The commonly used spectral clustering for image segmentation is the Shi-Malik Algorithm [12].

In this paper, we evaluate and compare nine segmentation methods which fall under the broad classification of thresholding, region and contour based segmentation and graph based clustering techniques. These algorithms are applied to dermoscopic images of skin lesions and the segmented results are evaluated by comparing with ground truth. Evaluation is by specificity, sensitivity, accuracy, border error, Hammoude distance, Hausdorff distance, MSE, PSNR and elapsed time values. The arrangement of paper is as follows - section 2 discusses the algorithms taken for evaluation, section 3 provides the experimental results and evaluation, section 4 discusses the results and concludes with section 5.

## 2. SEGMENTATION METHODS

The nine different segmentation techniques considered for comparison are:

- Global Thresholding (GT)
- Adaptive Thresholding (AT)
- K Means Clustering (KM)
- Fuzzy C Means (FCM)
- Expectation Maximization (EM)
- Statistical Region Merging (SRM)
- Active Contour Model(ACM)
- Chan Active Contour Model Without Edges(ACMWE)
- Spectral Clustering(SC)

### 2.1 GLOBAL THRESHOLDING

Global Thresholding is a technique where a single threshold value is applied throughout the image. GT is an iterative process which considers the mean of all pixels as the initial threshold, $T_0$. After grouping based on the selected threshold $T_0$, a new threshold (T) which is the average of the mean of pixel intensities of each group is calculated. The pixels are re-grouped based on T. This iterative process stops if the difference between the new threshold and the previous one is negligibly small [13].

Table.1. Algorithm for Global Thresholding

| | | |
|---|---|---|
| Input | : | Image (I) |
| Output | : | Segmented binary image |
| Steps | : | Set an initial threshold $T_0$ = mean ($\mu$) of all pixels<br>Subdivide the image based on $T_0$<br>Recompute T as, $T = (\mu_1 + \mu_2)/2$<br>Iterate until T converge |

This algorithm is relatively simple and generates good results for images with sharp peaks.

### 2.2 ADAPTIVE THRESHOLDING

Segmentation is based on a threshold value. Image is subdivided into small areas and averaged by a mean filter with appropriate window size. Each sub-image is segmented using different threshold values [1]. The output is a binary image showing the segmented regions.

Table.2. Algorithm for Adaptive Thresholding

| | | |
|---|---|---|
| Input | : | Image (I), window size (ws) |
| Output | : | Segmented binary image |
| Steps | : | Normalize and subdivide I with mean or median filter using ws<br>Compute threshold $T_i$ for each sub image, $i \epsilon I$<br>Compare each pixel with $T_i$<br>Assign to foreground or background based on the threshold |

Adaptive Thresholding performs well on images with uneven illumination.

### 2.3 K MEANS CLUSTERING

The objective of K means clustering [14] is to partition an image into mutually exclusive clusters by minimizing the distance metric between the pixel and the cluster centroid.

Table.3. Algorithm for K means clustering

| | | |
|---|---|---|
| Input | : | Image I with $X = \{x_1, x_2, \ldots, x_N\}$ pixels<br>$K = \{k_1, k_2, \ldots, k_K\}$ number of clusters |
| Output | : | Segmented image with K clusters |
| Steps | : | Randomly assign each pixel to any of the clusters<br>Compute the distance between the pixel and all centroids $C = \{c_1, .., c_K\}$ as<br>$\sum_{i=1}^{k} \sum_{X_j} \left\| X_j - C_k \right\|^2$ ; $x_j \epsilon k_i$<br>where $\|.\|$ denotes the Euclidean norm ,<br>$c_k$ = mean of all pixels in kth cluster<br>Reassign the pixel $x_j$ to the cluster $c_i$<br>Iff $\left\| X_j - C_i \right\|^2 \leq \left\| X_j - C_k \right\|^2$ ; $1 \leq k \leq K$<br>Repeat above steps until there is no further reassignment |

The number of clusters is fixed with a prior knowledge of the image. The distance between each pixel and all the cluster centroids including the one the pixel is located is calculated. Based on this distance metric, the pixels are reassigned to the nearest centroid. Thus a new centroid is calculated based on this reassignment of pixels. This iterative process continues until all the pixels have been grouped to their nearest centroid and the centroid values change no further. K means algorithm is easily programmable and computationally economical. The output is sensitive to initial choice of clusters [15].

## 2.4 FUZZY C MEANS

FCM is a soft computing technique [16] and a variant of K means.

Table.4. Algorithm for FCM

| | |
|---|---|
| Input | : Image I with $X = \{x_1, x_2, \ldots, x_N\}$ pixels<br>$C = \{c_1, c_2, \ldots, c_K\}$ number of clusters |
| Output | : Segmented image with C clusters |
| Steps | : Randomly assign each pixel to any of the clusters<br>Compute the degree of membership of each pixel to every cluster using<br>$u_{ij} = \dfrac{1}{\sum_{m=1}^{C} \dfrac{d_{ij}}{d_{im}\left(2/_{k-1}\right)}}$ where dij= $\lVert x_i - c_j \rVert$ (1)<br>Reassign the pixel, i to the cluster, *j* with which it has large $u_{ij}$ calculated using Eq.(1)<br>Compute the new cluster centre $c_j$ as<br>$C_j = \dfrac{\sum_{i=1}^{N} x_i u_{ij}^k}{\sum_{i=1}^{N} u_{ij}^k}$<br>Repeat until convergence |

Although FCM is an effective clustering technique, the resulting membership values do not always correspond well to the degree of belonging of the data, and it may be inaccurate in noisy environment.

## 2.5 EXPECTATION MAXIMIZATION

EM is a dual iterative procedure [17]. It assigns an initial mean ($\mu_0$), variance ($\sigma_0^2$) and prior probability ($p_0$) for each pixel belonging to a cluster. The initial values are

- $\mu_0$ - calculated with randomly chosen data points
- $\sigma_0^2$ - variance of full training set
- $p_0$ - assumed equal for all clusters
- E step - Gaussian probability distribution is applied to determine the pixel - cluster membership using Eq.(2)

$$P(X) = \frac{1}{\sqrt{2\pi\sigma^2}} e^{-(x-\mu)^2 / 2\sigma^2} \quad (2)$$

The likelihood of this probability is calculated as

$$l(\mu, \sigma^2; X_1, .., X_n) = \frac{n}{2} ln(2\pi) - \frac{n}{2} ln\,\sigma^2 - \frac{1}{2\sigma^2} \sum_{j=1}^{n} (X_j - \mu)^2 \quad (3)$$

- M step - The parameters (mean, variance and prior probability) are recalculated. With these values, the probability and the likelihood are recalculated. The algorithm terminates when the likelihood in the E step and M step merge.

Table.5. Algorithm for EM

| | |
|---|---|
| Input | : Image (I) , no. of clusters (k) |
| Output | : Image with k segments |
| Steps | : Initialize $\mu_0$, $\sigma_0^2$ and $p_0$ for each *k*<br>Compute the Gaussian probability using Eq.(2)<br>Compute log-likelihood using Eq.(3)<br>Recompute the 3 parameters; also Gaussian probability and log - likelihood<br>Iterate until maximum likelihood is achieved |

This algorithm is more flexible, since variance, mean and prior probabilities are taken into account.

## 2.6 STATISTICAL REGION MERGING

The Statistical Region Merging as proposed by Nock and Neilson [8] is a region merging segmentation technique where the merging of two or more regions is based on a statistical test. The statistical test is based on a predicate, which specifies the deviation in the intensities of the test regions. Thus the basic components of the SRM algorithm can be defined as merging predicate and order of merging. Any two regions (R and R') in an image I shall be merged if and only if they satisfy the following statistical test condition given in Eq.(4).

$$P(R, R') = \begin{cases} true; & |R - R'| \le \sqrt{b^2(R) + b^2(R')} \\ false; & otherwise \end{cases} \quad (4)$$

where, $b(R) = g\sqrt{\frac{1}{2Q}\left(\frac{1}{R} + \frac{1}{R'}\right) ln\frac{2}{\delta}}$

$$\delta = \frac{1}{6|I|^2}$$

Q - Quantification factor

The value of g is taken as 256. It is very important that the regions R and R' can be tested to get merged only if all the regions within R and R' have undergone the statistical test.

Table.6. Algorithm for SRM

| | |
|---|---|
| Input | : Color image (I) |
| Output | : Segmented image |
| Steps | : Sort the adjacent pixel pairs according to the increasing values of f(p, p') = $max_{a \in \{R,G,B\}} \lvert p_a' - p_a \rvert$<br>Apply the test condition over the successive regions as,<br>if $R(p_i) \neq R(p_i')$ and $P(R(p_i), R(p_i')) = true$ , then<br>merge the regions $R(p_i)$ and $R(p_i')$ |

The scale of segmentation increases with the value of Q. The algorithm has the advantage of speed and ease to implement. It could handle images with multiple channels, noisy and occluded images.

## 2.7 ACTIVE CONTOUR MODEL

The snake, $v(s) = \{x(s), y(s)\}$ is controlled by two energy terms – an internal energy and an external energy. This method [9] works by minimizing the energy functional, $E_{snake}$ which is defined as,

$$E_{snake} = E_{internal} + E_{external} + E_{constraint} \quad (5)$$

The final position of the snake will always have minimum energy. The internal energy is the sum of bending and elastic energy given by Eq.(6)

$$E_{internal} = E_{elastic} + E_{bending}$$

$$E_{internal} = \frac{1}{2}\int \alpha(s)|v_s|^2 ds + \frac{1}{2}\int \beta(s)|v_{ss}|^2 ds \tag{6}$$

where, $v_s$ and $v_{ss}$ - the first and second derivative of $v(s)$ respectively

$\alpha(s)$ – controls the elastic energy of the contour

$\beta(s)$ – controls the bending energy of the contour.

The external energy attracts the snake towards lines, edges and terminations. Given $I(x, y)$ is a gray level image, then the typical external energies are $-|\nabla \mathrm{I}(x,y)|^2$ or $-|\nabla(G_\sigma(x,y) * \mathrm{I}(x,y))|^2$ where $G_\sigma$ is the 2D Gaussian function with standard deviation σ and ∇ is the gradient operator .

The snake that minimizes $E_{snake}$ must satisfy the following Euler equation

$$\alpha V_{ss} - \beta V_{ssss} - \nabla E_{external} = 0 \tag{7}$$

Table.7. Algorithm for ACM

| | | |
|---|---|---|
| Input | : | Image, I; Contour points |
| Output | : | Segmented Image |
| Steps | : | Specify the initial contour<br>Compute the internal energy and the external energy<br>Minimize the Euler Lagrange's equation, Eq.(7) iteratively |

The major pitfalls in this model are that the capture range of the snake is limited and hence requires expert initialization; the snakes do not detect curvatures in the image.

## 2.8 ACTIVE CONTOUR MODEL WITHOUT EDGES

Chan Vese model, a special case of Mumford Shah segmentation technique is an iterative algorithm to detect smooth and discontinuous edges. Its main objective is to minimize the energy functional given as

$$\begin{aligned} F(c_1,c_2,C) = \mu L(C) + vA(in(C)) + \lambda_1 \int_{in(C)} |u_0(x,y) - c_1|^2 dxdy \\ + \lambda_2 \int_{out(C)} |u_0(x,y) - c_2|^2 dxdy \end{aligned} \tag{8}$$

where, $\mu, v \geq 0$; $\lambda_1 = \lambda_2 = 1$ are the positive weighting parameters

$u_0(x,y)$ - input image

$c_1$, $c_2$ - average inside and outside the contour respectively

$\mu L(C) + vA(in\ (C))$ - Regularizing term

$$\begin{aligned} F_1(C) + F_2(C) = \lambda_1 \int_{in(C)} |u_0(x,y) - c_1|^2 dxdy \\ + \lambda_2 \int_{out(C)} |u_0(x,y) - c_2|^2 dxdy \end{aligned} \tag{9}$$

F1(C), F2(C)-fitting terms

The values of $c_1$ and $c_2$ are calculated using the Heaviside function H (φ) as in Eq.(10) and Eq.(11)

$$c_1(\phi) = \frac{\int_\Omega u_0(x,y) H(\phi(x,y)) dxdy}{\int_\Omega H(\phi(x,y)) dxdy} \tag{10}$$

$$c_2(\phi) = \frac{\int_\Omega u_0(x,y)(1 - H(\phi(x,y))) dxdy}{\int_\Omega (1 - H(\phi(x,y))) dxdy} \tag{11}$$

The corresponding level–set formulation of Eq.(8) in terms of the gradient descent, φ is given as

$$\frac{\partial \phi}{\partial t} = \delta(\phi)\left[\mu k(\phi)|\nabla \phi| - v - \lambda_1 (u_0 - c_1)^2 + \lambda_2 (u_0 - c_2)^2\right] \tag{12}$$

where, δ(ϕ) - Dirac delta function

(ϕ) - mean curvature of the contour

$\nabla(\phi)$ - gradient of the contour.

The evolution is solved using finite differences and the final contour is obtained when $\frac{\partial \phi}{\partial t}$ is minimum.

Table.8. Algorithm for ACM without edges

| | | |
|---|---|---|
| Input | : | Input image I |
| Output | : | Segmented Image |
| Steps | : | Initialize mask for contour, ϕ, 0<br>Calculate $c_1$ and $c_2$<br>Compute the Fitting term $F_1(C)$ + $F_2(C)$ and the energy functional $\frac{\partial \phi}{\partial t}$<br>Iterate until $\frac{\partial \phi}{\partial t}$ is minimum |

This algorithm has the advantage of detecting smooth boundaries. It automatically changes the topology and is highly resistive to noises.

## 2.9 SPECTRAL CLUSTERING

Normalized cuts algorithm or Normalised Spectral Clustering as proposed by Shi and Malik partitions points into disjoint clusters by calculating the eigen vectors of laplacians using similarity matrix. Given a set of points X = $\{x_1, x_2, \ldots. x_n\}$, similarity graphs shall be constructed either by $\epsilon$ - neighbourhood graph, k-nearest neighbor graph or fully connected graph [11]. The adjacency matrix using Gaussian similarity function is given in Eq.(13).

$$W_{ij} = e^{-\|x_i - x_j\|^2 / 2\sigma^2};\ i \neq j \text{ and } W_{ii} = 0 \tag{13}$$

$$D_{ii} = \textstyle\sum_j W_{ij} \tag{14}$$

The unnormalized Laplacian matrix is

$$\mathrm{L} = \mathrm{D} - \mathrm{W} \tag{15}$$

The normalized symmetric and random walk Laplacian matrix are given in Eq.(16) and Eq.(17)

$$L_{sym} = I - D^{-1/2} W D^{-1/2} \tag{16}$$

$$L_{rw} = I\text{-}D^{-1}W \qquad (17)$$

where, $W_{ij}$ –affinity matrix and $D_{ii}$-diagonal matrix

Table.9. Algorithm for SC

| | | |
|---|---|---|
| Input | : | Image (I), No. of clusters(k) |
| Output | : | Segmented Image |
| Steps | : | Define an adjacency matrix, W using Eq.(13)<br>Construct graph laplacian using Eq.(15)<br>Compute the column matrix U containing the first k eigenvectors $u_1,\ldots..u_k$<br>Choose the k smallest eigenvalue as the k eigen vectors to define k dimensional subspace<br>Use k means to form clusters in this subspace |

SC obtains data representation in a low-dimensional space that can be easily clustered

## 3. EXPERIMENTAL RESULTS AND EVALUATION

This section provides the experimental results of the above specified algorithms for the dermoscopic images. The algorithms are evaluated using the following metrices [3], [18]

- Accuracy
- Specificity
- Sensitivity
- Border Error
- Hammoude distance
- Hausdorff distance
- Mean Square Error (MSE)
- Peak Signal to Noise ratio (PSNR)
- Elapsed time

Accuracy - It is the proportion of true results (both true positives and true negatives) in the population.

$$Accuracy = \frac{\#(TP)+\#(TN)}{\#(TP)+\#(TN)+\#(FP)+\#(FN)}$$

Specificity - It is the proportion of actual negatives which are correctly identified as such.

$$Specificity = \frac{\#(TN)}{\#(TN)+\#(FP)}$$

Sensitivity - It is the proportion of positives measured as such.

$$Sensitivity = \frac{\#(TP)}{\#(TP)+\#(FN)}$$

Hammoude distance - It makes a pixel by pixel comparison enclosed by the two boundaries.

$$Hammoude\ distance = \frac{\#(FP)+\#(FN)}{\#(TN)}$$

Hausdorff distance - It finds the largest distance between the boundary points.

Hausdorff distance = max{max$_i$d(gt$_i$, SR), max$_i$d(sr$_i$, GT)}

Border Error - It is the ratio of the area covered by the XOR of segmented result (SR) and ground truth (GT) images to the area covered by GT image.

$$Border\ error = \frac{(FP)+(FN)}{(TP)+(FN)}$$

MSE - It measures the average of the square of the difference between the segmented image and the original image.

$$MSE = \frac{1}{n}\sum_{i=1}^{n}\left(I\_seg_i - I\_orig_i\right)^2$$

PSNR - It is a measure of reconstruction quality.

$$PSNR = 10\,log_{10}\frac{max\,imum\ intensity^2}{MSE}$$

Elapsed time - It is the total time taken for the completion of the program

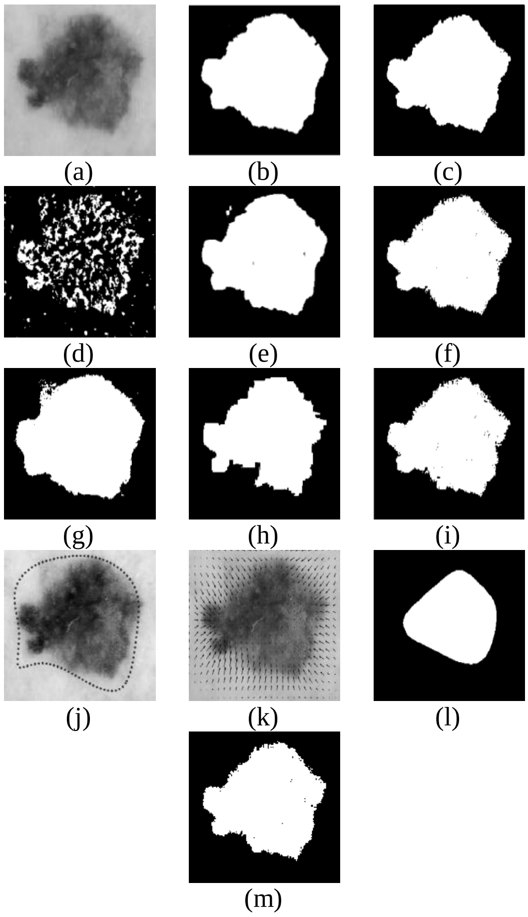

Fig.1(a). Original image, (b). Ground truth and Segmented outputs for (c). GT, (d). AT, (e). KM, (f). FCM, (g). EM, (h). SRM, (i). ACMWE, (j). ACM – initial contour, (k). ACM – External force field, (l). ACM, (m). SC

Table.10. Evaluation table for algorithms

| Methods | Sensitivity (%) | Accuracy (%) | Border Error (%) | Specificity (%) | Hammoude Distance | Hausdorff Distance | MSE (%) | PSNR (%) | Elapsed Time (s) |
|---|---|---|---|---|---|---|---|---|---|
| **GT** | 91.09 | 95.16 | 22.21 | 96.25 | 7.61 | 4.64 | 0.05 | 63.09 | 1.15 |
| **AT** | 47.18 | 77.41 | 81.86 | 92.76 | 38.84 | 8.09 | 0.23 | 55.28 | 0.11 |
| **KM** | 83.41 | 90.7 | 28.13 | 94.28 | 17.71 | 5.99 | 0.09 | 60.56 | 0.20 |
| **FCM** | 90.99 | 96.39 | 13.79 | 98.55 | 6.03 | 4.7 | 0.04 | 63.86 | 0.20 |
| **EM** | 93.52 | 95.63 | 15.82 | 96.39 | 7.64 | 4.64 | 0.04 | 63.61 | 1.87 |
| **SRM** | 85.83 | 95.35 | 17.1 | 98.5 | 7.57 | 5.86 | 0.05 | 62.36 | 0.77 |
| **ACM** | 39.84 | 82.28 | 63.56 | 99.68 | 29.47 | 6.6 | 0.18 | 56.1 | 0.35 |
| **ACMWE** | 90.84 | 95.62 | 21.78 | 97.64 | 6.92 | 4.97 | 0.04 | 62.62 | 6.56 |
| **SC** | 90.75 | 96.42 | 13.39 | 98.98 | 6.09 | 4.43 | 0.04 | 64.03 | 22.73 |

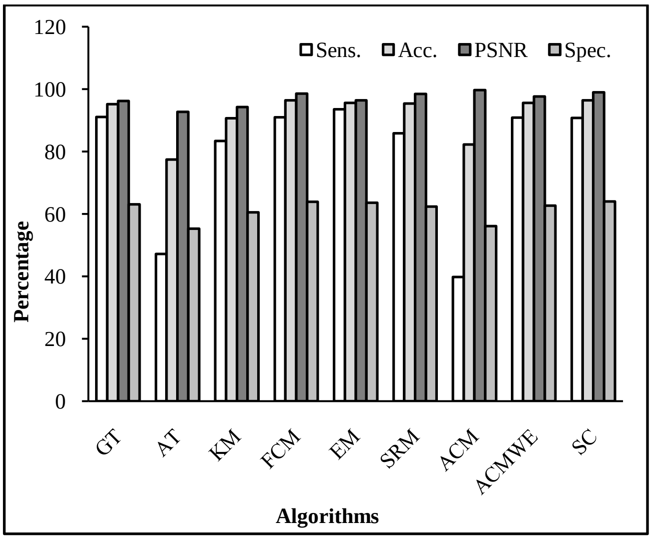


Fig.2. Comparison of to-be-maximum parameters

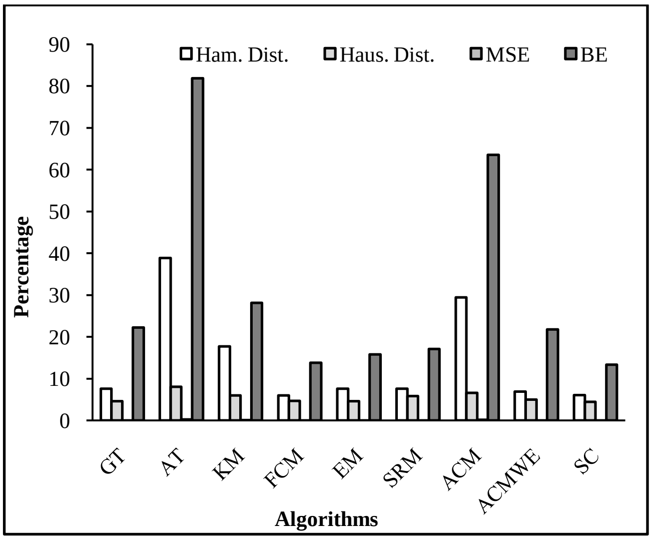


Fig.3. Comparison of to-be-minimum parameters

## 4. DISCUSSION

Images are preprocessed using median filter. The segmented output of the algorithms implemented in MATLAB is shown in Fig.1 and the mean of the evaluation metrices is tabulated in Table.10. The database of 20 images from [19] was processed using all the methods under evaluation. AT provides better results only when there is significant color change between the skin and lesion. The overall efficiency of the algorithms with user interaction, not only depends on the efficiency of the algorithm but also on the user's expertise to give the input. For example, the snake model (ACM) outputs are influenced by the shape of initial contour and the speed with which the user specifies the contour. Though ACMWE provides good results, it takes more time for computation. The overall results show that FCM provides better results for dermoscopic images with comparatively minimum computational time. Even though with Spectral Clustering, the segmentation process consumes considerably higher time, the border error is minimized in comparison with other algorithms.

## 5. CONCLUSION

This paper evaluates and analyses the effectiveness of some of the segmentation algorithms over dermoscopic images. The result of each algorithm is greatly influenced by the type of image used for analysis. All algorithms do not generate same range of results for all kind of images. Hence we have to choose algorithms specific to the image type. The overall results show that the fuzzy clustering as well as Spectral Clustering algorithms gives better results for dermoscopic images. Even though, both algorithms provide comparable results Fuzzy Clustering algorithm segments faster.

## REFERENCES

[1] R. C. Gonzalez and R. E. Woods, "*Digital Image Processing*", Second Edition, Englewood Cliffs, NJ: Prentice -Hall, 2002.

[2] Nikil Pal and Sankar Pal, "A review on image segmentation techniques", *IEEE Transactions on Pattern Recognition*, Vol. 26, No. 9, pp. 1277-1294, 1993.

[3] Margarida Silveira, Jacinto C. Nascimento, Jorge S. Marques, André R. S. Marçal, Teresa Mendonça, Syogo Yamauchi, Junji Maeda and Jorge Rozeira, "Comparison of Segmentation Methods for Melanoma Diagnosis in Dermoscopy Images", *IEEE Journal of Selected Topics in Signal Processing*, Vol. 3, No. 1, pp. 35-45, 2009.

[4] J. B. MacQueen, "Some Methods for classification and analysis of multivariate observations", *Proceedings of the Fifth Berkeley Symposium on Mathematical Statistics, and Probability*, Vol. 1, pp. 281-297, 1997.

[5] James C Bezdeck, Robert Ehrlich and William Full, "FCM - The Fuzzy c-means Clustering Algorithm", *Computers and Geoscience*, Vol. 10, No. 2-3, pp. 191-203, 1984.

[6] G. C. Karmakar, L. Dooley and S. M. Rahman, "A survey of fuzzy rule based image segmentation techniques", *First IEEE Pacific-Rim Conference on Multimedia*, pp. 350-353, 2000.

[7] R. Nock and F. Nielsen, "Statistical region merging", *IEEE Transactions on Pattern Analysis and Machine Intelligence*, Vol. 26, No. 11, pp. 1452-1458, 2004.

[8] F. Nielsen and R. Nock, "On region merging: The statistical soundness of fast sorting, with applications", *IEEE International Conference on Computer Vision and Pattern Recognition*, Vol. 2, pp. 19-26, 2003.

[9] M. Kass, A. Witkin and D. Terzopoulos, "Snakes: Active contour models", *International Journal on Computer Vision*, Vol. 1, pp. 321-331, 1987.

[10] Tony F Chan and Luminita Vese, "Active contour model without edges", *IEEE Transactions on Image Processing*, Vol. 10, No. 2, pp. 266-277, 2001.

[11] Ulrike Von Luxburg, "A tutorial on spectral clustering", *Statistics and computing*, Vol. 17, No. 4, pp. 395-416, 2007.

[12] Jianbo Shi and Jitendra Malik, "Normalized Cuts and Image Segmentation", *IEEE Transactions on Pattern Analysis and Machine Intelligence*, Vol. 22, No. 8, pp. 888-905, 2000.

[13] P. K. Sahoo and S. Soltani and A. K. C. Wong, "A survey of thresholding techniques", *Computer Vision, Graphics and Image Processing*, Vol. 41, No. 2, pp. 233-260, 1988.

[14] Emre Celebi, "Improving the performance of K means for color quantization", *Journal on Image and Vision computing*, Vol. 29, No. 4, pp. 260-271, 2011.

[15] Emre Celebi, "Deterministic initialization of k - means using hierarchical clustering", *International Journal of Pattern Recognition and Artificial Intelligence*, Vol. 26, No. 7, pp. 1-23, 2013.

[16] Yang Zhang and Chung Fu-Lai, "Robust fuzzy clustering-based image segmentation", *Applied Soft Computing*, Vol. 9, No. 1, pp. 80-84, 2009.

[17] Todd. K. Moon, "The Expectation Maximization Algorithm", *IEEE Signal Processing Magazine*, Vol. 13, pp. 47-60, 1996.

[18] Amir Reza Sadri, Maryam Zekri, Saeid Sadri, Niloofar Ghaisari, Mojgan Mokhtari and F. Kolahdouzan, "Segmentation of Dermoscopy Images Using Wavelet Networks", *IEEE Transactions on Biomedical Engineering*, Vol. 60, No. 4, pp. 1134-1141, 2013.

[19] http://www.dermnetnz.org/doctors/dermoscopy-course/images/index.html.